Available online at www.sciencedirect.com
ScienceDirect
Journal of Computational Physics 226 (2007) 494–508
JOURNAL OF COMPUTATIONAL PHYSICS
www.elsevier.com/locate/jcp

A discrete calculus analysis of the Keller Box scheme and a generalization of the method to arbitrary meshes

J.B. Perot *, V. Subramanian

University of Massachusetts, Amherst, Mechanical and Industrial Engineering, Amherst, MA 1003, United States

Received 16 January 2007; received in revised form 17 April 2007; accepted 20 April 2007
Available online 29 April 2007

Abstract

The Keller Box scheme is a face-based method for solving partial differential equations that has numerous attractive mathematical and physical properties. It is shown that these attractive properties collectively follow from the fact that the scheme discretizes partial derivatives exactly and only makes approximations in the algebraic constitutive relations appearing in the PDE. The exact discrete calculus associated with the Keller Box scheme is shown to be fundamentally different from all other mimetic (physics capturing) numerical methods. This suggests that a unique exact discrete calculus does not exist. It also suggests that existing analysis techniques based on concepts in algebraic topology (in particular – the discrete de Rham complex) are unnecessarily narrowly focused since they do not capture the Keller Box scheme. The discrete calculus analysis allows a generalization of the Keller Box scheme to non-simplectic meshes to be constructed. Analysis and tests of the method on the unsteady advection–diffusion equations are presented.

Keywords: Discrete calculus; Keller Box; Mimetic; Numerical methods

1. Introduction

The Keller Box scheme [1] is also sometimes referred to as the Preissman Box scheme [2]. It is a variation of the finite volume approach in which unknowns are stored at control volume faces rather than at the more traditional cell centers. The name alludes to the fact that in space–time, the unknowns sit at the corners of the space–time control volume – which is a box in one space dimension on a stationary mesh. The original development of the method [1,2] dealt with parabolic initial value problems such as the unsteady heat equation. The method was made better known by Cebeci and Bradshaw [3,4] as a method for the solution of the boundary layer equations. Since that time the approach has been extended to address convection [5,6] and to the Euler and Navier–Stokes compressible equations [7–9]. Some mixed finite element methods [10–12] place some of the degrees of freedom on the element faces (rather than on the vertices). This is a similar idea, however mixed FE

* Corresponding author. Tel.: +1 413 545 3925; fax: +1 413 545 1027.
E-mail address: perot@ecs.umass.edu (J.B. Perot).

0021-9991/$ - see front matter
doi:10.1016/j.jcp.2007.04.015

methods never place all the degrees of freedom on the faces, making the Box schemes a unique approach without a direct FE analog.

Recently there has been a renewed interest in the Box method for the solution of wave equations. This is, in part, due to the fact that the method has been shown to be *multisimplectic* [13] and that it propagates all waves in the correct direction [14]. These are formal mathematical statements indicating what has been understood intuitively by practitioners for some time – that the method captures the physics of PDEs well. In Section 2, we present an analysis that explains why this method captures physics well. In essence the argument will be that the Box method can be formulated in such a way that all the calculus is exact. In the Box method all approximations lie in the constitutive equations (which are also physical approximations). Errors in material properties do not affect the physical properties of a PDE system – such as energy conservation and wave propagation.

Numerical methods that 'capture physics well' are sometimes referred to as 'mimetic' [15,29]. Their discrete differential operators mimic the essential properties (integration by parts, orthogonality, etc.) of the continuous differential operators (div, grad, and curl). Staggered mesh methods [16] and some of their unstructured variants [17–19] are mimetic, as are face and edge elements [20,21]. Recent work has shown how to generate higher-order mimetic methods [22] and how to derive mimetic methods [23] – rather than show that a method is mimetic (or not) after it has been formulated. Section 2 uses the discrete calculus analysis to show that the Keller Box scheme is also mimetic. The most interesting observation from Section 2 is that the underlying exact discrete calculus for the Box scheme is different from that of all other known mimetic methods.

The classical Keller Box method is only applicable to simplectic meshes (line segments in 1D, triangles in 2D, and tetrahedra in 3D). This is because the unknowns (such as temperature and normal heat flux for the heat equation) are located at cell faces whereas the control volume equations and constitutive relation for the heat flux are discretized on the cells. The number of unknowns and equations only match on a simplectic mesh. Section 3 describes this numerical issue in detail and presents a generalization of the method to arbitrary meshes.

It will be demonstrated that the Box scheme is always partially implicit in time and requires a matrix inversion to advance the solution. The fact that the Keller Box discretization is fully coupled at each time step is a reflection of the physics of parabolic systems – which are also fully coupled. This attribute is mathematically and physically reflective of the PDE system but the matrix inversion can be numerically problematic. A minor issue is the fact that Keller Box matrix system is not symmetric. Far more disconcerting is the fact that iterative solution techniques do not work. This is because the residuals do not correspond directly with the unknowns for which a solution is sought. Residual redistribution does not work. It solves a different (and usually singular and therefore ill-defined) problem. The difficulty with using iterative methods may explain why the method is not more popular in practice. The generalization of the Box method presented in Section 3 overcomes all these numerical difficulties.

The accuracy and efficiency of the generalized Box scheme is tested in Section 4 where a number of problems are solved and results are compared with other mimetic and classical finite volume schemes. Section 5 presents a brief summary and discussion of the results.

2. Discrete calculus analysis of the classic Keller Box scheme

The face-based discretization approach (Box scheme) about to be described can be used to discretize any PDE. A number of examples are listed in Section 1. However, for clarity of presentation and illustration we will focus on a particular equation system – the unsteady diffusion equation (or heat equation).

$$\frac{\mathrm{d}(\rho C T)}{\mathrm{d}t} = \nabla \cdot k \nabla T + S \tag{1}$$

In heat transfer, the temperature T is the fundamental unknown, and the material parameters are, k the conductivity, ρC the heat capacity and S the source term. This equation, or slight variants of it, finds application in many other fields of science and engineering with different physical interpretations for the variables. The presentation should therefore be accessible to a wide variety of readers.

It is convenient to consider the heat equation in an expanded form that clearly separates the physics/mathematics from the material constitutive approximations.

$$\frac{\mathrm{d}i}{\mathrm{d}t} + \nabla \cdot \mathbf{q} = S \quad \text{Conservation of energy} \tag{2a}$$

$$\mathbf{g} = \nabla T \quad \text{Definition of gradient} \tag{2b}$$

$$\mathbf{q} = -k\mathbf{g} \quad \text{Fourier's law} \tag{2c}$$

$$i = \rho C T \quad \text{Perfectly Caloric material} \tag{2d}$$

This formulation introduces two new variables, i internal energy per unit volume, and $\mathbf{q}$ the heat flux. The last two equations are algebraic constitutive relations. They are approximations for how some materials behave and they are not exact – even physically. Discrete calculus methods place all numerical errors/approximations in these last two (material) equations. The first two equations, containing the physics and calculus will be discretized exactly. The advantage of discretizing the physics and calculus exactly is that the resulting numerical methods and discrete solutions cannot violate any physical or mathematical principles. All numerical errors manifest themselves as errors in the material properties – not the physics. We note that discretization, the process of making a PDE into a finite system of equations and unknowns, can always be performed exactly. But solution of that exact discrete system (which has more unknowns than equations) always requires some sort of interpolation/approximation.

2.1. Exact discretization

The discretization of the energy equation (Eq. (2a)) is just the classic control volume approach. Integrating over each mesh cell (in space and time) gives the exact discrete equation:

$$\int_c i\,\mathrm{d}V\Big|^{n+1} + \sum_f \int_{t^n}^{t^{n+1}} \mathrm{d}t \int_f \mathbf{q}\cdot\mathbf{n}\,\mathrm{d}A = \int_c i\,\mathrm{d}V\Big|^{n} + \int_{t^n}^{t^{n+1}} \mathrm{d}t \int_c S\,\mathrm{d}V \tag{3a}$$

There is one equation for each cell. The discrete unknowns in this equation are, $I_c = \int_c i\,\mathrm{d}V$ the total energy in the cell, and $Q_f = \int_{t^n}^{t^{n+1}} \mathrm{d}t \int_f \mathbf{q}\cdot\mathbf{n}\,\mathrm{d}A$ the time integrated heat flux between the cells (or on the domain boundary). Beyond the exact time integration and recognizing that the fundamental unknowns are integral quantities, not point values, there is little difference from classic control volume formulations thus far. The key difference in the Box scheme (and other mimetic schemes) lies in the discretization of Eq. (2b).

Exact discretization of Eq. (2b) can be achieved by integrating Eq. (2b) over the cell volume just like the energy equation. This gives the exact discrete equation

$$\int_c \mathbf{g}\,\mathrm{d}V = \int_c \nabla T\,\mathrm{d}V = \sum_f \int_f T\hat{\mathbf{n}}_f\,\mathrm{d}A = \sum_f \mathbf{n}_f \overline{T}_f \tag{3b}$$

where $\hat{\mathbf{n}}_f$ is the outward pointing normal vector for each face and $\mathbf{n}_f = A_f\hat{\mathbf{n}}_f$ is the outward normal times the face area. The last equality in this equation assumes cell faces are planar and the normal vector can be removed from the integral. The fundamental unknowns in this exact vector equation on each cell are again integral quantities. $\overline{T}_f = \frac{1}{A_f}\int_f T\,\mathrm{d}A$ is the average temperature on the cell face and $\frac{1}{V_c}\int_c \mathbf{g}\,\mathrm{d}V = \mathbf{g}_c$ is the average temperature gradient vector in each cell.

It is to be noted that other possibilities exists for discretizing equation (2b) exactly. In fact, all other known mimetic methods use $\int \mathbf{g}\cdot\mathrm{d}\mathbf{l} = \int \nabla T\cdot\mathrm{d}\mathbf{l} = T_2 - T_1$ where the integral is a line integral connecting two cell centers (cell-based methods) or two cell vertices (node-based methods) and the temperature unknown is a point value located at the end points of the line. This approach is extensively reviewed in Perot and Subramanian [23]. Higher-order finite volume versions of this approach are described by [22]. Finite element versions of this approach are referred to as edge elements (for the node-based lines) or face elements (for the cell-based lines) [20,21].

Eq. (3b) is, therefore, a unique exact discretatization approach. It is remarkable because it shows that there is not a single exact discrete calculus (and its dual) as the works of Marsden and coworkers [26,27] implicitly

suggest. It is also important because this approach can be analyzed using the discrete calculus approach (it is an exact discretization) but it cannot be analyzed using the methods from discrete algebraic topology regularly applied in the analysis of face and edge finite elements (in particular, the Box discretization operators do not satisfy a discrete de Rham complex).

In linear algebraic terms, the exact discretization in Eqs. (3a) and (3b) can be written as:

$$I_c^{n+1} + DQ_f = I_c^n + \overline{S}_c V_c \Delta t \tag{4a}$$

$$V_c \mathbf{g}_c = N\overline{T}_f \tag{4b}$$

where the divergence operator D and the normal operator N are defined as:

$$DQ_f = \sum_f Q_f \tag{5}$$

$$N\overline{T}_f = \sum_f \mathbf{n}_f \overline{T}_f \tag{6}$$

It is emphasized that the discretizations in Eqs. (4a) and (4b) are exact and no approximations have been introduced so far. Exact discretization of the physics and calculus is the fundamental underlying reason why this method has attractive physical and mathematical properties. In essence, the method has no choice but to behave well since the math and physics are exact.

2.2. Constitutive equation interpolations

Note, however, that the exact discrete equations (4a) and (4b) are not closed or solvable. In order to solve the system, the constitutive equations (2c) and (2d) must be included. Closure of the system requires relating the heat flux $Q_f = \int_{t^n}^{t^{n+1}} \mathrm{d}t \int_f \mathbf{q}\cdot\mathbf{n}\,\mathrm{d}A$ to the cell average temperature gradient $\mathbf{g}_c = \frac{1}{V_c}\int_c \mathbf{g}\,\mathrm{d}V$, and the average temperature at the faces $\overline{T}_f$ to the total energy in the cells $I_c = \int_c i\,\mathrm{d}V$. These quantities reside in different places (both in space and time) and are different in number. So the constitutive relations are inherently interpolation problems that involve some sort of approximation. The interpolation problem can be performed many different ways. Different interpolations can lead to finite volume, finite difference, or finite element looking methods. The Keller Box scheme is the simplest and most obvious interpolation choice – piecewise constant and linear functions in the cells. The general idea of placing errors into the constitutive equations is suggested in Stanley [28].

In order to relate Q_f to $\mathbf{g}_c$, Eq. (2c) is integrated over each cell and the conductivity is assumed piecewise constant within each cell:

$$\int_c \mathbf{q}\,\mathrm{d}V = -k_c \int_c \mathbf{g}\,\mathrm{d}V = -k_c V_c \mathbf{g}_c \tag{7a}$$

Assuming the heat flux is piecewise constant within each cell relates the average flux to its boundary values:

$$\int_c \mathbf{q}\,\mathrm{d}V = \mathbf{q}_c V = \sum_f \mathbf{r}\int_f \mathbf{q}\cdot\mathbf{n}\,\mathrm{d}A \tag{7b}$$

where $\mathbf{r}$ is the position vector pointing from the cell center to the face center (i.e. $\mathbf{r} = \mathbf{x}_f - \mathbf{x}_c$). This identity is a result of applying the divergence theorem to the quantity $\nabla\cdot(\mathbf{xq})$ and assuming $\nabla\cdot\mathbf{q}$ is constant within each cell. Note that the relation (7b) is a spatially first-order approximation for the flux vector that is valid for any polyhedral cell shape. First-order approximation of the flux is sufficient to allow second-order spatial accuracy for the temperature solution.

Combining Eqs. (7a) and (7b) and using the operator R to denote the operation $RQ_f = \sum_f \mathbf{r}Q_f$ gives the final (and approximate) discrete version of Fourier's law

$$RQ_f = -k_c V_c \Delta t[\alpha \mathbf{g}_c^{n+1} + (1-\alpha)\mathbf{g}_c^n] \tag{8}$$

The gradient must be numerically integrated over the time interval. A value of $\alpha = \frac{1}{2}$ gives second-order accuracy in time (the trapezoidal integration rule). A value of $\alpha = 1$ uses a first-order fully implicit integration.

In order to relate I_c to $\overline{T}_f$ Eq. (2d) is also integrated over each cell:

$$I_c = \int_c i \, \mathrm{d}V = \int_c \rho c T \, \mathrm{d}V \tag{9a}$$

Since the heat flux is assumed constant in the cell and the conductivity is assumed to be constant, it is assumed that the temperature is linearly varying within each cell (which assumes Fourier's law holds). If the heat capacity is also assumed to be constant then

$$\int_c \rho c T \, \mathrm{d}V = (\rho c)_c \overline{T}_c V_c = (\rho c)_c \sum_f V_{fc} \overline{T}_f \tag{9b}$$

where V_{fc} is the volume formed by the cell face connected with the cell center of gravity (Fig. 1). For triangles, tetrahedra, rectangles, and right angled hexahedra $V_{fc} = \frac{1}{\mathrm{NF}_c} V_c$, where NF_c is the number of cell faces. Employing the averaging operator $A\overline{T}_f = \frac{1}{\mathrm{NF}_c} \sum_f \overline{T}_f$ (or for general polyhedra $A\overline{T}_f = \frac{1}{V_c} \sum_f V_{fc} \overline{T}_f$) and combining Eqs. (9a) and (9b) gives

$$I_c = (\rho c)_c V_c A\overline{T}_f \tag{10}$$

Combining the exact discrete physics/math equations (4a) and (4b), and the discrete constitutive equations (8) and (10) the complete discrete system may be written as:

$$(\rho c V)_c A\overline{T}_f^{n+1} + DQ_f = (\rho c V)_c A\overline{T}_f^{n} + \Delta t V_c \overline{S}_c^{n+1/2} \tag{11a}$$

$$\alpha \Delta t k_c N \overline{T}_f^{n+1} + RQ_f = -(1-\alpha)\Delta t k_c N \overline{T}_f^{n} \tag{11b}$$

This can be written in matrix form as:

$$\begin{bmatrix} (\rho c V)_c A & D \\ \alpha \Delta t k_c N & R \end{bmatrix} \begin{Bmatrix} \overline{T}_f^{n+1} \\ Q_f \end{Bmatrix} = \begin{Bmatrix} (\rho c V)_c A\overline{T}_f^{n} + \Delta t V_c \overline{S}_c^{n+1/2} \\ -(1-\alpha)\Delta t k_c N \overline{T}_f^{n} \end{Bmatrix} \tag{12}$$

Note that a fully explicit Box scheme ($\alpha = 0$) is not possible because the matrix becomes singular (the submatrix N is not square). As mentioned in Section 1, the Box scheme always requires a matrix to be inverted. The time level for Q_f does not exist because this variable is actually an average of the face normal heat flux over the time interval.

It is important to observe that while Eq. (11a) is a scalar equation, Eq. (11b) is actually a vector equation because the operators N and R contain vectors. Hence, the system Eq. (12) contains $(d+1)\mathrm{NC}$ equations, where d is the spatial dimensionality of the problem (usually 2 or 3) and NC is the total number of cells in the domain. The system given by Eq. (12) has 2NF unknowns, where NF is the total number of faces in the domain (the average temperature at time $n+1$ and the average normal heat flux over the interval). In order to solve the system, equations for the boundary conditions on the domain faces must be imposed. On boundary faces an equation for either the average temperature (Dirichlet) or the average heat flux (Neumann) must be imposed. The full system to be solved then becomes

$$\begin{bmatrix} (\rho c V)_c A & D \\ \alpha \Delta t k_c N & R \\ I_{Db} & 0 \\ 0 & I_{Nb} \end{bmatrix} \begin{Bmatrix} \overline{T}_f^{n+1} \\ Q_f \end{Bmatrix} = \begin{Bmatrix} (\rho c V)_c A\overline{T}_f^{n} + \Delta t V_c \overline{S}_c^{n+1/2} \\ -(1-\alpha)\Delta t k_c N \overline{T}_f^{n} \\ \overline{T}_b \\ Q_b \end{Bmatrix} \tag{13}$$

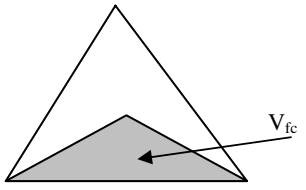

Fig. 1. Shaded region represents the volume V_{fc} within the 2D triangular cell.

It is clear that even mixed (Robin) boundary conditions can be easily included in this type of framework (though we have not added that level of complexity in this example). The matrix I_{Db} is NF wide but only the number of Dirichlet boundary faces (NFD) high. It has zeros everywhere but a single 1 in each column corresponding to a Dirichlet boundary face. Similarly I_{Nb} is NF wide but only number of Neumann boundary faces (NFN) high and has a single 1 in the column corresponding to Neumann boundaries and is zero elsewhere.

The system (Eq. (13)) now has NFD + NFN + $(d+1) * \mathrm{NC}$ equations and 2NF unknowns. In the case of simplices (where the number of faces for each cell is $d+1$) the number of equations and unknowns is now equal and the matrix problem has a unique solution, as indicated by the numerical tests. On general polyhedral meshes, there are more unknowns than equations and multiple possible solutions exist.

3. General implementation of the Box method

The restriction of the Box scheme to simplectic meshes is actually a minor problem compared with the difficulty associated with inverting the matrix. The matrix is square, and non-singular, so in principal there is no problem and Gauss elimination will always work. However, in practice, Gauss elimination (or any direct method) is not a feasible way to invert a large sparse matrix. For complex 2D domains, almost any 3D domain, or for unsteady solutions, iterative solvers are a far better choice. Unfortunately, unlike almost all other discretization methods, the Box method does not result directly in matrices that are amenable to iterative solution techniques. In this section, we will show how this problem can be fixed so that the method can be applied to practical problems.

3.1. Arbitrary meshes and iterative inversion

Most numerical methods generate matrices in which each unknown has a closely associated discrete equation located at the same place in the mesh. Iterative methods then calculate the error in the equation (the residual) and use that to correct the solution estimate. Such a procedure clearly does not work for the Box scheme where there are $d+1$ residuals on each cell, and the unknowns (two of them) are situated on the faces. Arbitrary residual distribution, where the $d+1$ cell residuals are distributed to neighboring faces in some logical (but fundamentally *ad hoc*) manner does not work. Not only is residual distribution arbitrary and non-unique, it solves a different (essentially preconditioned) problem that is almost invariably singular (rank deficient) due to the averaging nature of distribution process.

As the unknowns are located at the faces, it is desirable to have the equations constructed at the faces as well. A rational and well posed way to accomplish this is weight each equation by a diagonal matrix $\mathbf{W}$ and then to premultiply Eq. (13) by its transpose

$$\mathbf{M}^{\mathrm{T}}\mathbf{W}\mathbf{M}u = \mathbf{M}^{\mathrm{T}}\mathbf{W}b \tag{14}$$

Since $\mathbf{M}$ converts face quantities into cell quantities, $\mathbf{M}^{\mathrm{T}}$ converts cell quantities into face quantities. This weighted least squares approach solves most of the numerical issues associated with the Box scheme. The matrix to be inverted is now symmetric and positive semi-definite. General meshes where the matrix $\mathbf{M}$ is not square are now turned into a square system. Most importantly, the residuals and unknowns now have corresponding locations and the system is amenable to iterative solution methods.

The matrix $\mathbf{M}^{\mathrm{T}}$ is

$$\mathbf{M}^{\mathrm{T}} = \begin{bmatrix} A^{\mathrm{T}}(\rho c V)_c & N^{\mathrm{T}}(\alpha \Delta t k_c) & I_{Db}^{\mathrm{T}} & 0 \\ -G & R^{\mathrm{T}} & 0 & I_{Nb}^{\mathrm{T}} \end{bmatrix} \tag{15}$$

The transpose operators are given the following definitions:

$$A^{\mathrm{T}}T_c = \frac{1}{\mathrm{NF}_{c1}}T_{c1} + \frac{1}{\mathrm{NF}_{c2}}T_{c2} \tag{16a}$$

$$N^{\mathrm{T}}\mathbf{q} = (\mathbf{q}_{c1} - \mathbf{q}_{c2}) \cdot \mathbf{n}_f \tag{16b}$$

$$GT_c = T_{c2} - T_{c1} \tag{16c}$$

$$R^{\mathrm{T}}\mathbf{q} = \mathbf{q}_{c1}\cdot\mathbf{r}_1 - \mathbf{q}_{c2}\cdot\mathbf{r}_2 \tag{16d}$$

The actual matrix $\mathbf{M}^{\mathrm{T}}\mathbf{W}\mathbf{M}$ is never actually constructed. Most iterative solvers function as long as the matrix-vector product can be calculated. The matrix multiply is performed in three separate stages. This keeps the connectivity information very simple – only face to cell connectivity is required. It also keeps the number of mathematical operations down since the sparcity of the component matrices is far less than that of their product. Nevertheless, the full matrix

$$\begin{bmatrix} A^{\mathrm{T}}(\rho cV)_c^2 W_1 A + N^{\mathrm{T}}(\alpha\Delta t k_c)^2 W_2 N + I_{Db}^{\mathrm{T}} W_D I_{Db} & A^{\mathrm{T}}(\rho cV)_c W_1 D + N^{\mathrm{T}}(\alpha\Delta t k_c) W_2 R \\ -G(\rho cV)_c W_1 A + R^{\mathrm{T}}(\alpha\Delta t k_c) W_2 N & -G W_1 D + R^{\mathrm{T}} W_2 R + I_{Wb}^{\mathrm{T}} W_W I_{Wb} \end{bmatrix}$$

does indicate how the weights should be chosen. Each term in the matrix entries should have the same units as the other terms in that entry or the system can become ill condition artificially. Since the variable $\overline{T}_f^{n+1}$ has units of temperature (°C), and the flux Q_f has units of energy (J), this means that $(\rho cV)_c$ has units of entropy (J/C) and $(\alpha\Delta t k_c)$has units of entropy flux times length $\left(\frac{J}{Cm^2}m\right)$. This shows that the weights should be chosen with the following dimensional scaling: $W_1 = I$, $W_2 = 1/L_c^2$, $W_D = (\rho cV)_c^2$, and $W_W = I$, where L_c is a characteristic length of each mesh cell (such as the cell volume divided by the cell surface area).

The matrix $I_{Db}^T W_D I_{Db}$ is a square matrix with values on the diagonal locations corresponding to Dirichlet boundary faces and 0s everywhere else. In order to enforce the Dirichlet boundary conditions exactly allow $W_D \to \infty$. This limit only affects the Dirichlet boundary faces and is equivalent to setting the boundary temperature to its given value. A similar affect happens for the Neumann boundaries and the heat flux values there. Residuals corresponding to those boundary unknowns are then zero. In an iterative solver, such as conjugate gradients, the vector entries corresponding to the boundary condition locations are set to zero for a simple matrix multiply. For a residual calculation, the boundary values are set to their prescribed values.

The dimensionless variable $\frac{(\alpha\Delta t k_c)V_c}{(\rho cV)_c L_c^2}$ is a mesh Peclet number and should be less than O(1) to achieve temporal accuracy.

3.2. General physics – advection

To simplify the presentation, the general face-based method was developed thus far without including the advection term. This section demonstrates the ease with which additional physics can now be included into the basic approach.

With advection the conservation law Eq. (2a) is written

$$\frac{\mathrm{d}i}{\mathrm{d}t} + \nabla\cdot(i\mathbf{u}) + \nabla\cdot\mathbf{q} = S \tag{17}$$

In the discrete calculus approach this equation was integrated over space and time. The advection term then becomes

$$\int_{t^n}^{t^{n+1}} \mathrm{d}t \int_c \nabla\cdot(i\mathbf{u})\mathrm{d}V = \sum_f \int_{t^n}^{t^{n+1}} \mathrm{d}t \int_f i\mathbf{u}\cdot\mathbf{n}\,\mathrm{d}A = \sum_f F_f^i \tag{18}$$

which is exact, but introduces a new variable, $F_f^i = \int_{t^n}^{t^{n+1}} \mathrm{d}t \int_f i\mathbf{u}\cdot\mathbf{n}\,\mathrm{d}A$, the time integrated energy flux through each cell face. We note that these fluxes are related to the unknowns in the time derivative which are integrals of the internal energy at a fixed time and over the volume, $(I_c = \int_c i\,\mathrm{d}V)$. The advection fluxes are at the 'sides' of the space–time control volume and the I_c are evaluated at the top and bottom faces of the space–time control volume. Eq. (18) is exact but not closed. The constitutive relation for the internal energy and some interpolation approximations must be invoked to close these terms. One possibility is

$$F_f^i = \sum_f \frac{\rho c U_f^{n+1/2}}{A_f} \int_{t^n}^{t^{n+1}} \mathrm{d}t \int_f T\,\mathrm{d}A = \sum_f (\rho c)_f^{n+1/2} U_f^{n+1/2} \Delta t\left(\beta\overline{T}_f^{n+1} + (1-\beta)\overline{T}_f^n\right) \tag{19}$$

This assumes that the normal velocity and heat capacity are constant in space and time on the face. It also assumes a simple time integration rule ($\beta = \frac{1}{2}$ is trapezoidal, $\beta = 0$ is explicit Euler). In the Keller Box scheme the spatial integration is exact and does not require an approximation. The heat capacity and velocity flux are assumed to be known. Many discrete calculus implementations for the Navier–Stokes equations (such as staggered mesh schemes) have the velocity flux on the faces as the primary variable, so the velocity flux will often not require any approximation.

The matrix **M** (including implicit convection) may now be written as

$$\mathbf{M} = \begin{bmatrix} (\rho c V)_c A + \beta \Delta t D (\rho c U)_f & D \\ \alpha \Delta t k_c N & R \\ I_{Db} & 0 \\ 0 & I_{Nb} \end{bmatrix} \tag{20}$$

The Keller Box method does not result in a symmetric matrix anyway, so implicit advection does not add an extra numerical burden.

4. Numerical tests of accuracy and cost

Given the unusual nature of the Keller Box scheme it is of some interest to see how it compares with more standard control volume schemes in both its accuracy and computational cost. This section will therefore compare the proposed method with the classical finite volume approach on a number of test cases. Also of interest is to see how the face-based method proposed in this paper compares with other methods derived using the discrete calculus approach. Hence, the comparisons also include cell-based and node-based discrete calculus methods. These methods are derived by Perot and Subramanian [23].

A direct comparison of accuracy is difficult when comparing node-based, face-based and cell-based methods. Hence, our ultimate metric of method performance in this work will be level of accuracy obtained per the computational cost. This section first presents a commonly used cell-based finite volume method, which is then used for comparison against the discrete calculus methods. Numerical tests illustrating the spatial and temporal accuracy as well as the cost to obtain a desired accuracy are then presented. In all the subsequent plots, the following legends are consistently used – face for the Keller Box-like DC method proposed in this paper, mixed for the cell-based DC method, node for the node-based DC method (these methods are derived in [23]) and FV for the classical finite volume method (described in Section 4.1).

4.1. Cell-based finite volume method

Given the restrictions of space and time we will restrict our attention to cell-based finite volume methods. These methods also use the conservation equation $\frac{d(\rho C V T_c)}{dt} + D Q_f = 0$, where T_c is typically located at the cell centroid and Q_f is the heat flux at the mesh faces. The key in these methods is to relate the face flux Q_f, to the cell temperature, T_c. In order to account for strong mesh distortions, typically a flux corrected scheme is employed that relates the heat flux and temperature as

$$Q_f = \mathbf{q}_f \cdot \mathbf{n}_f - (kGT + \mathbf{q}_f \cdot \mathbf{d}) \frac{\mathbf{d} \cdot \mathbf{n}_f}{\mathbf{d} \cdot \mathbf{d}} \tag{21}$$

where $\mathbf{d} = \mathbf{x}_{c2} - \mathbf{x}_{c1}$ and the face heat flux vector $\mathbf{q}_f = -(w_1 k_1 \nabla T_1 + w_2 k_2 \nabla T_2)$ is constructed using an estimate of the temperature gradient computed as

$$\nabla T = \frac{1}{V_c} \int_c \nabla T \, dV = \frac{1}{V_c} \sum_f T_f \mathbf{n}_f \tag{22}$$

where the face average temperature $T_f = w_1 T_{c1} + w_2 T_{c2}$ is obtained by a weighted average of the cell temperatures. Choosing volume weights, $w_1 = V_1/(V_1 + V_2)$ results in a method where the face flux satisfies Gauss' theorem on the domain containing both cells touching that face, and the face value is linearly interpolated

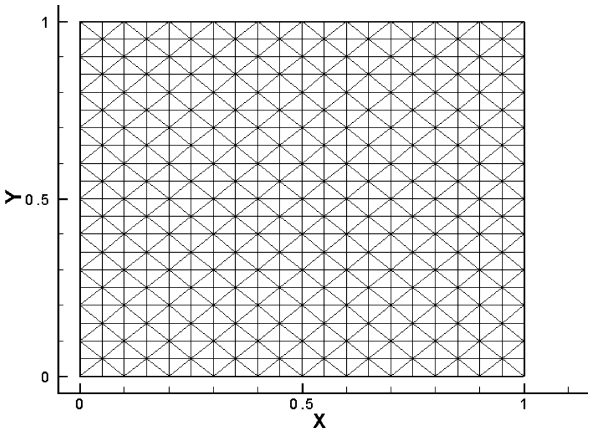

Fig. 2. Mesh with different diffusivities on either side of the interface ($x = 0.5$).

between the two cell values using the perpendicular distances (which is equivalent to assuming no variation in the cell temperatures tangential to the face).

4.2. Discontinuous conductivity at an angle

This problem is taken from Shashkov [24] and Morel et al. [25]. Although the theory for discontinuous coefficients only implies that the normal component of heat flux should be continuous, many numerical methods also assume that tangential flux components are continuous at a discontinuity. Such methods will have difficulties when solving for conduction that occurs at an angle to the discontinuity.

The mesh (shown in Fig. 2) is divided into two different materials with different diffusivities along the interface $x = 0.5$. Note that the discontinuity in the material is captured by the mesh. The diffusion coefficients are defined as

$$k = \begin{cases} k_1 & 0 < x < 0.5 \\ k_2 & 0.5 < x < 1 \end{cases} \tag{23}$$

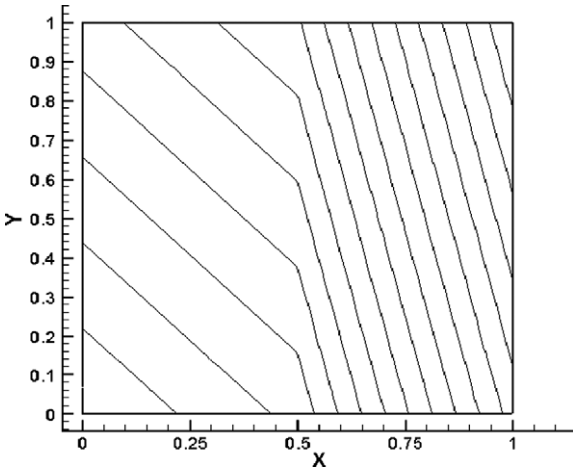

Fig. 3. Isolines of temperature contours obtained by the discrete calculus methods.

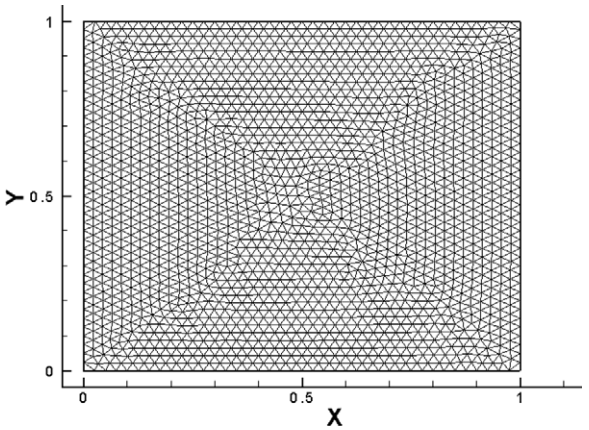

Fig. 4. Typical mesh used for convergence study.

The exact steady state solution is

$$T = \begin{cases} a + bx + cy & 0 \leqslant x \leqslant 0.5 \\ a - b\frac{k_1 - k_2}{2k_2} + b\frac{k_1}{k_2}x + cy & 0.5 < x \leqslant 1 \end{cases} \tag{24}$$

This problem has a discontinuity in the tangential flux at the material interface. The normal component of the flux (bk_1) is the same across the entire domain. However, the tangential flux component is $k_1 c$ on the left side and $k_2 c$ on the right side of the interface. The numerical experiments employ $a = b = c = 1$, $k_1 = 4$ and $k_2 = 1$. Dirichlet boundary conditions derived from the analytical answer are applied at the boundaries.

The temperature isolines obtained using the discrete calculus methods for this problem are shown in Fig. 3. The solutions obtained by all the discrete calculus methods agree with the exact answer to machine precision. This not only confirms that the discrete calculus methods are exact for linear functions but also illustrates the physics capturing behavior of these methods. The classical finite volume method fails to capture the solution exactly.

4.3. Spatial accuracy on a non-linear problem

In this test, the spatial accuracy of the face-based Keller Box-like discrete calculus method (face) is compared with a cell-based FV method (Section 4.1) and two other DC methods (node and mixed derived in [23]) in a steady-state heat diffusion problem with a uniform source term $S = 4$ and unit conductivity ($\nabla \cdot (-k\nabla T) = S$). The typical mesh employed is shown in Fig. 4. Dirichlet boundary conditions are imposed on the left and right boundaries, and homogeneous Neumann boundary conditions are imposed on the top and bottom boundaries. The exact solution $T(x) = 2x^2 - 2x$ is a quadratic function. The spatial accuracy is plotted in Fig. 5.

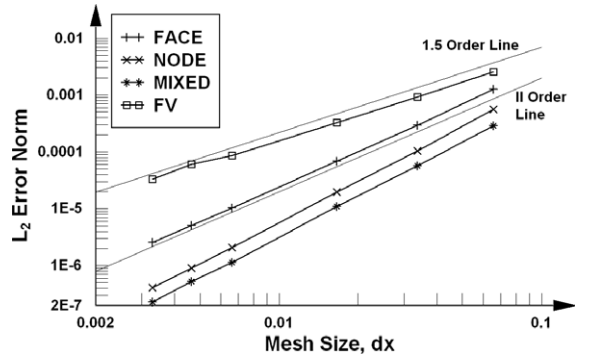

Fig. 5. Spatial accuracy of DC methods compared with the FV method.

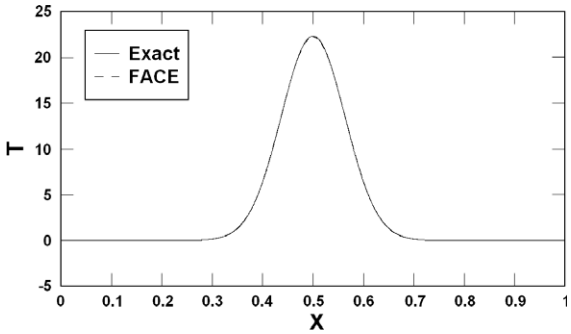

Fig. 6. Solution to the unsteady diffusion problem at $t = 0.002$ on a 2D mesh.

It is noted that while the finite volume method (FV) shows a rate of convergence of approximately 1.5, all the discrete calculus methods (face, node, and mixed) consistently show second-order convergence. For a particular mesh, the other DC methods are more accurate than the Keller Box method, which is, in turn, more accurate than the classical finite volume scheme.

4.4. Temporal accuracy

While any time advancement scheme can be used with the face-based discrete calculus method, treating the diffusion term in a fully implicit manner would lead to a first-order temporal accuracy. In order to obtain a second-order temporal accuracy, it is preferable to employ the trapezoidal rule, which is obtained by employing $\alpha = 0.5$ in Eq. (13).

In this test, an unsteady diffusion equation is solved on the mesh shown in Fig. 4. The initial conditions and boundary conditions are specified as follows:

$$\begin{aligned} \text{ICs} \quad & T(x,t_0) = \tfrac{1}{\sqrt{t_0}} \exp\left\{-\tfrac{(x-0.5)^2}{4kt_0}\right\}; \quad Q_f(x,t_0) = \tfrac{(x-0.5)n_x}{2t_0\sqrt{t_0}} \exp\left\{-\tfrac{(x-0.5)^2}{4kt_0}\right\} \\ & x = 0 \quad T(t) = 0 \\ & x = 1 \quad T(t) = 0 \\ \text{BCs} \quad & y = 0 \quad \tfrac{\partial T(t)}{\partial y} = 0 \\ & y = 1 \quad \tfrac{\partial T(t)}{\partial y} = 0 \end{aligned} \tag{25}$$

In Eq. (25), n_x refers to the x-component of the face normal vector at each face and k refers to the diffusivity (chosen as unity for this problem). The initial time t_0 is chosen as 0.001 and the simulation is run up to a final time of $t = 0.002$. The analytical solution to this problem is $T(x,t) = \frac{1}{\sqrt{t}} \exp\{-(x-0.5)^2/4kt\}$. The simulation is run with

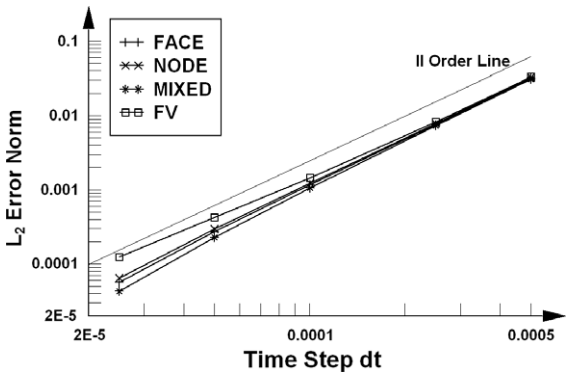

Fig. 7. Temporal accuracy of DC methods compared with the FV method.

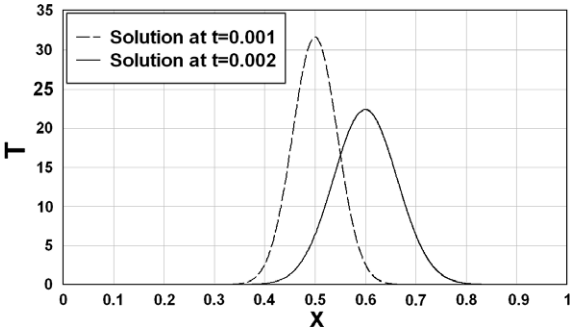

Fig. 8. Solution to the unsteady advection–diffusion problem at $t = 0.002$.

various values of the time step (dt) and the L2 norm of the error is computed at the same final time, $t = 0.002$. The result is plotted in Fig. 7, which confirms the second-order temporal accuracy of all the discrete calculus methods. The computed solution is compared with the exact answer at $t = 0.002$ in Fig. 6. It is seen from Fig. 7 that the temporal order of accuracy of the finite volume method is initially close to two but reduces as the mesh is refined.

4.5. Accuracy on an advection–diffusion problem

In this section, the face-based DC method is applied to solve an advection–diffusion equation. The same mesh shown in Fig. 4 is used and the initial and boundary conditions are specified as follows:

$$\begin{aligned}
&\text{ICs} \quad T(x,t_0) = \tfrac{1}{\sqrt{t_0}} \exp\left\{-\tfrac{(x-ut-0.4)^2}{4kt_0}\right\};\\
&\qquad\quad Q_f(x,t_0) = \tfrac{(x-ut-0.4)n_x}{2t_0\sqrt{t_0}} \exp\left\{-\tfrac{(x-ut-0.4)^2}{4kt_0}\right\}\\
&\text{BCs} \quad x = 0 \quad T(t) = 0\\
&\qquad\quad x = 1 \quad T(t) = 0\\
&\qquad\quad y = 0 \quad \tfrac{\partial T(t)}{\partial y} = 0\\
&\qquad\quad y = 1 \quad \tfrac{\partial T(t)}{\partial y} = 0
\end{aligned} \tag{26}$$

A constant velocity of $u = 100$ m/s was chosen for the advection term. In Eq. (26), n_x refers to the x-component of the face normal vector at each face and k refers to the diffusivity (chosen as unity for this problem). The initial time t_0 is chosen as 0.001 and the simulation is run up to a final time of $t = 0.002$. The analytical solution to this problem is $T(x,t) = \frac{1}{\sqrt{t}} \exp\{-(x-ut-0.4)^2/4kt\}$. The initial and final states of the solution are shown in Fig. 8. The simulation is run with various values of the time step (dt) and the L2 norm of the error is computed at the same final time, $t = 0.002$ and plotted in Fig. 9 for the DC and FV methods.

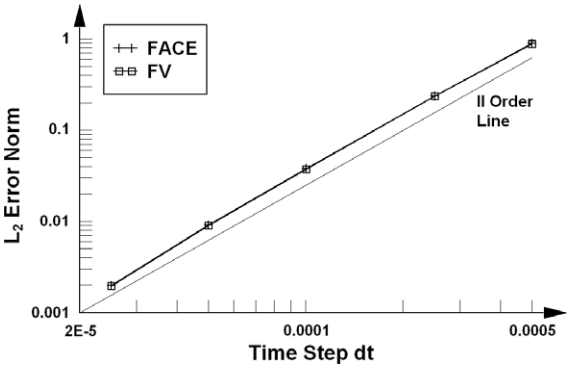

Fig. 9. Temporal accuracy of DC methods compared with the FV method.

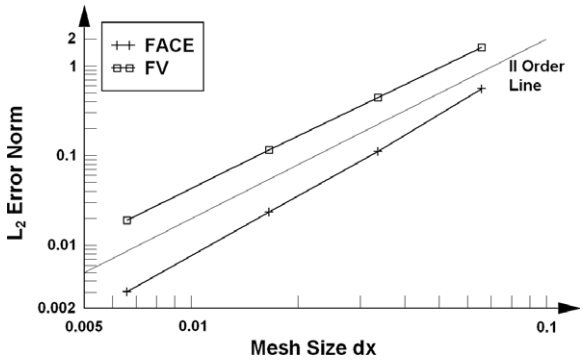

Fig. 10. Spatial accuracy of DC methods compared with the FV method.

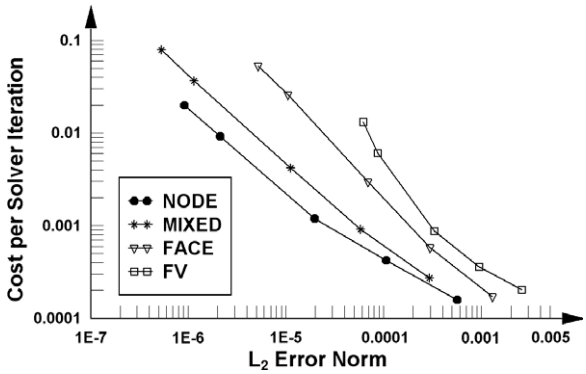

Fig. 11. Cost to obtain a desired accuracy.

Second-order temporal accuracy is observed for both the methods. The FV method also displays second-order accuracy since the convection term (which dominates in this problem) is second-order accurate in the FV formulation as well. However, a spatial accuracy comparison between the two methods, obtained at the same final time $t = 0.002$ indicates that the discrete calculus method is more accurate and shows a slightly larger convergence rate than the FV method (see Fig. 10).

4.6. Cost to achieve a desired accuracy

Although the discrete calculus methods were shown to be more accurate than the traditional lower order methods in the previous tests, it might be more important to compare the cost-effectiveness of the discrete calculus methods against the classical finite volume method. Hence, the computational cost (in terms of the CPU time) per solver iteration is plotted against the L2 error norm in Fig. 11 for the problem considered in Section 4.3, which really compares the cost incurred for a desired accuracy level. It is observed that for any given accuracy level the discrete calculus methods are always more cost-effective than the traditional method. Also, it is clearly seen that the cost for the finite volume method tends to increase more rapidly than the discrete calculus methods as the need for accuracy increases. However, it must be kept in mind that the total cost to obtain convergence may be higher for the face-based DC method than the FV method, especially because of the high condition number of the system presented in Eq. (14). A good preconditioner may partly alleviate this issue.

5. Summary

The Keller Box scheme has been rederived using the discrete calculus approach in an attempt to explain the desirable mathematical and physical properties of the method. As a result of this derivation, the method has

been generalized to arbitrary meshes. It has been noted that the exact discretization of the gradient equation in this method is a volume integral as opposed to a line integral used in the other discrete calculus (or edge/face FE) methods, indicating that there is not a unique discrete calculus. It has been demonstrated that the Keller Box scheme is always partially implicit in time and requires a matrix inversion at every time step. The issue that the classical Keller Box method cannot be solved using iterative methods has been solved in this work using a weighted least squares technique. Such a technique also results in a symmetric matrix so that a fast conjugate gradient algorithm can be used to obtain a solution. It has been demonstrated that the resulting discrete calculus method shows second-order spatial and temporal accuracy on generic unstructured meshes and that the computational cost per solver iteration to obtain a desired accuracy is lower compared to classical finite volume schemes but somewhat higher than other mimetic schemes.

Acknowledgments

We thank Jason Frank at CWI, Amsterdam, for first bringing the Keller Box scheme to our attention and for initially posing the fundamental question behind this work. Partial financial support for this work was provided by the Office of Naval Research (N00014-01-1-0267), the Air Force Office of Scientific Research (FA9550-04-1-0023) and the National Science Foundation (CTS-0522089).

References

[1] H.B. Keller, A new difference scheme for parabolic problems, in: B. Hubbard (Ed.), Numerical Solutions of Partial Differential Equations II, Academic Press, New York, 1971, pp. 327–350.
[2] A. Preissman, Propagation des intumescences dans les canaux et rivieres, 1st Congres de l'Assoc Francaise de Calc, AFCAL, Grenoble, 1961, pp. 433–442.
[3] T. Cebeci, K.C. Chang, P. Bradshaw, Solution of a hyperbolic system of turbulence-model equations by the ''box'' scheme, Comput. Meth. Appl. Mech. Eng. 22 (1980) 213.
[4] P. Bradshaw, T. Cebeci, J.H. Whitelaw, Engineering Calculation Methods for Turbulent Flow, Academic Press, 1981.
[5] J.-P. Croisille, Keller's box-scheme for the one-dimensional stationary convection–diffusion equation, Computing 68 (1) (2002) 37–63.
[6] J.-P. Croisille, I. Greff, An efficient box-scheme for convection–diffusion equations with sharp contrast in the diffusion coefficients, Comput. Fluids 34 (2005) 461–489.
[7] J.-J. Chattot, A conservative box-scheme for the Euler equations, Int. J. Numer. Meth. Fluids 31 (1999) 149–158.
[8] J.-J. Chattot, Box-schemes for first order partial differential equations, Adv Comp Fluid Dynamics, Gordon and Breach, New York, 1995, pp. 307–331.
[9] S.F. Wornom, M.M. Hafez, Calculation of quasi-one-dimensional flows with shocks, Comput. Fluids 14 (2) (1986) 131–140.
[10] G.F. Carey, W.F. Spotz, Higher order mixed methods, Commun. Numa. Meth. Eng. 13 (1997) 553–564.
[11] B. Courbet, J.-P. Croisille, Finite volume box-schemes on triangular meshes, Math. Model. Numer. Anal. 32 (1998) 631–649.
[12] J.-P. Croisille, Finite volume box-schemes and mixed methods, Math. Model. Numer. Anal. 34 (2000) 1087–1106.
[13] Th.J. Bridges, S. Reich, Multi-symplectic integrators: numerical schemes for Hamiltonian PDEs that conserve symplecticity, Phys. Lett. A 284 (2001) 184–193.
[14] J. Frank, B. Moore, S. Reich, Linear PDEs and numerical methods that preserve a multi-symplectic conservation law, SIAM J. Sci. Comput. 28 (2006) 260–277.
[15] J.M. Hyman, M. Shashkov, The orthogonal decomposition theorems for mimetic finite difference methods, SIAM J. Numer. Anal. 36 (3) (1999) 788–818.
[16] F.H. Harlow, J.E. Welch, Numerical calculations of time dependent viscous incompressible flow of fluid with a free surface, Phys. Fluids 8 (12) (1965) 2182–2189.
[17] R. Nicolaides, X. Wu, Covolume solutions of three-dimensional div–curl equations, SIAM J. Numer. Anal. 34 (1997) 2195–2203.
[18] Roy Nicolaides, Da-Qing Wang, A higher order Covolume method for planar div–curl problems, Int. J. Numer. Meth. Fluids 31 (1) (1999) 299–308.
[19] J.C. Cavendish, C.A. Hall, T.A. Porsching, A complementary volume approach for modeling three-dimensional Navier–Stokes equations using dual Delaunay/Voronoi tessellations, Int. J. Numer. Meth. Heat Fluid Flow 4 (1994) 329–345.
[20] J.-C. Nedelec, Mixed finite elements in R3, Numer. Math. 50 (1980) 315–341.
[21] P.A. Raviart, J.M. Thomas, A Mixed Finite Element Method for Second Order Elliptic Problems, Springer Lecture Notes in Mathematics, vol. 606, Springer Verlag, 1977, pp. 292–315.
[22] V. Subramanian, J.B. Perot, Higher order mimetic methods for unstructured meshes, J. Comput. Phys. 219 (2006) 68–85.
[23] J.B. Perot, V. Subramanian, Discrete calculus methods for diffusion, J. Comput. Phys. (2006), doi:10.1016/j.jcp.2006.12.022.
[24] M. Shashkov, S. Steinberg, Solving diffusion equations with rough coefficients in rough grids, J. Comput. Phys. 129 (1996) 383–405.
[25] J.M. Morel, J.E. Dendy Jr., M.L. Hall, S.W. White, A cell-centered Lagrangian-mesh diffusion differencing scheme, J. Comput. Phys. 103 (1992) 286.

[26] A.N. Hirani, Discrete exterior calculus. Ph.D. Thesis Caltech, May 2003, http://resolver.caltech.edu/CaltechETD:etd-05202003-095403.
[27] M. Desbrun, A.N. Hirani, M. Leok, J.E. Marsden, Discrete Exterior Calculus, 2005, arXiv.org:math/0508341.
[28] S. Stanley, The accuracy of numerical models for continuum problems, in: H. Bulgak, C. Zenger (Eds.), Error Control and Adaptivity in Scientific Computing, NATO Science Series, Series C: Mathematical and Physical Sciences, vol. 536, 1999, pp. 299–323. Available from: <http://www.math.unm.edu/~stanly/prints/publications.html>.
[29] J.M. Hyman, S. Steinberg, The convergence of mimetic discretization for rough grids, Comput. Math. Appl. 47 (10–11) (2004) 1565–1610.